Mechanical Properties and Morphology of Polyethylene–Polypropylene Blends with Controlled Thermal History

JUN LI,[1] ROBERT A. SHANKS,[1] YU LONG[2]

[1] Department of Applied Chemistry, RMIT University, Melbourne, Victoria 3001, Australia

[2] CSIRO Manufacturing Science and Technology, Clayton, Victoria 3168, Australia

ABSTRACT: The effect of time–temperature treatment on the mechanical properties and morphology of polyethylene–polypropylene (PE–PP) blends was studied to establish a relationship among the thermal treatment, morphology, and mechanical properties. The experimental techniques used were polarized optical microscopy with hot-stage, scanning electron microscopy (SEM), differential scanning calorimetry (DSC), and tensile testing. A PP homopolymer was used to blend with various PEs, including high-density polyethylene (HDPE), low-density polyethylene (LDPE), linear low-density polyethylene (LLDPE), and very low density polyethylene (VLDPE). All the blends were made at a ratio of PE:PP = 80:20. Thermal treatment was carried out at temperatures between the crystallization temperatures of PP and PEs to allow PP to crystallize first from the blends. A very diffuse PP spherulite morphology in the PE matrix was formed in partially miscible blends of LLDPE–PP even though PP was present at only 20% by mass. Droplet-matrix structures were developed in other blends with PP as dispersed domains in a continuous PE matrix. The SEM images displayed a fibrillar structure of PP spherulite in the LLDPE–PP blends and large droplets of PP in the HDPE–PP blend. The DSC results showed that the crystallinity of PP was increased in thermally treated samples. This special time–temperature treatment improved tensile properties for all PE–PP blends by improving the adhesion between PP and PE and increasing the overall crystallinity. In particular, in the LLDPE–PP blends, tensile properties were improved enormously because of a greater increase in the interfacial adhesion induced by the diffuse spherulite and fibrillar structure. © 2000 John Wiley & Sons, Inc. J Appl Polym Sci 76: 1151–1164, 2000

Key words: polypropylene and polyethylene blends; thermal treatment; tensile properties; crystal structure; spherulite

INTRODUCTION

Polypropylene (PP) is a commercially important polymer; however, its poor impact strength at low temperature and poor environmental stress-cracking resistance has set limitations to its applications. These properties of PP can be improved by either the incorporation of ethylene during copolymerization or mechanical blending with polyethylene (PE).[1] Propylene–ethylene copolymers give better performance than does PP at low temperatures. However, these copolymers require controlled, specialized polymerization during manufacture and, therefore, they are more expensive. Thus, blending of PP and PE is an economic alternative.

Various PEs have been used to modify PP: high-density polyethylene (HDPE),[2–8] low-density polyethylene (LDPE),[6–11] linear low-density PE (LLDPE),[12–15] and, more recently, very low and ultralow density polyethylene (VLDPE and ULDPE)[16] and ultrahigh molecular weight HDPE (UHMWPE).[17,18] Most polymer pairs are immiscible due to an unfavorable free energy of mixing, and their applications are limited by a lack of desirable mechanical properties resulting from poor interfacial adhesion and poor stress transfer between individual phases. The morphology and mechanical properties of PE–PP blends have already been studied extensively.[2–20] This is because of the considerable commercial interest in pursuing better performance of these blends and the scientific interest in the relationship between the morphology and properties of PE–PP blends. The properties of polymer blends not only depend on polymer characteristics, but also on the composition ratio, the method of compounding and processing, as well as the thermal history of the material.

Different mechanical behavior has been reported for apparently similar blend systems.[2–4,6,19] Linear additive properties of pure PP and PE in the modulus and yield stress were observed in HDPE–PP blends by some authors,[6] while others reported a large positive deviation[2–4] or negative deviation[19] from linearity. The synergism in the modulus and yield stress has been attributed to a reduction in the average spherulite size of PP and an increase in overall crystallinity introduced by the addition of PE and an increase in tie molecules or intercrystalline links observed by scanning electron microscopy (SEM).[3] Negative deviation may be ascribed to the loss of cohesion of the immiscible inclusions in a matrix. It has also been postulated that a small amount of PE may decrease the PP matrix plasticity, and the PE has a marked reinforcing effect resulting in a delay in neck formation, and, hence, an increase in the yield stress.[5] Elongation at break, in all cases, has been found to be markedly decreased for the blends compared with homopolymers.[2–8]

Synergism in mechanical properties has been observed in HDPE–PP blends but not in LDPE–PP blends.[6–11] This was attributed to the closeness of the melting temperature of HDPE and PP.[20] A later study by Lee et al.[8] compared the properties and morphologies of HDPE–PP and LDPE–PP blends. Rheology measurements and morphology studies showed that the interfacial adhesion between PP and HDPE was better than that between PP and LDPE, even though both the HDPE–PP and LDPE–PP binary blends were typical immiscible systems.

Dumoulin et al.[12,13] studied the rheology and tensile properties of LLDPE–PP blends. The melt rheology indicated a partial miscibility of the LLDPE–PP blends. The Young's modulus showed negative deviation in the LLDPE-rich region and positive deviation at PP concentrations of 50% or higher from the simple rule of mixtures. The yield stress and strain at yield showed negative deviation. Conversely, other workers reported positive deviations from the additivity rule for tensile strength[15] and yield strength[14] and a linear relationship between the modulus and composition.[14] Overall, blends of LLDPE–PP have superior behavior to that of LDPE–PP blends.

The reason for the different results obtained on similar systems is that the grade of the polymers and the methods of making blends are different. In PE–PP blends, the viscosity ratio of the polymers has profound effects on the blend performance. This was demonstrated by Bains and Balke,[21] who showed that when viscosities of LLDPE and PP were more closely matched, an increase up to 50% in tensile strength and modulus was observed over the rule of mixtures line. SEM analysis showed a more diffuse interface between the component phases. In contrast, blends where the component viscosities were very different showed tensile properties either slightly above or below the rule of mixtures line. Similar results were reported by Lee et al.[16] on ULDPE–PP blends. The method of compounding and processing has a profound effect on the blend properties. It was noted that samples prepared by compression molding were less ductile and less strong than those prepared by injection molding.[9,22] An increase in the mixing time and intensity improved the degree of dispersion; however, prolonged or intensive mixing also increased the thermal and mechanical degradation. There is an optimum mixing procedure that should be sought.[23,24]

The effect of annealing on the mechanical properties of PE–PP blends was also studied.[19,25,26,27] Varin and Djokovic found that annealing at 135°C for 5 h of injection-molded HDPE–PP blends improved the modulus and yield stress at the cost of elongation at break.[19] Similar results were reported by Blom and co-workers[25] on the annealed HDPE–PP blends at 75°C for 7 days. This is because annealing improves the crystallinity and interfacial adhesion between phases in

Table I   List of Materials

Code Name	Comonomer	MFI [g $(10 \text{ min})^{-1}$]	Source
PP	—	28	Orica
LLDPE1	5 mol % hexene	1	Orica
LLDPE2	5 mol % hexene	2.5	Orica
LDPE	—	20	Kemcor Australia
HDPE	—	22	Mobil
VLDPE	6.3 mol % butene	27	Kemcor

the PE–PP blends. Lin et al.[26] reported that annealing at 165 and 155°C improved the interfacial adhesion between PP and ethylene–propylene copolymers. The peel strength increased with increasing annealing temperature and time. This was attributed to the interdiffusion through the interface and entanglement of molecules with each other during annealing. The longer the annealing time, the greater the number of entanglements and, therefore, the interface will thicken in the sandwichlike sample. Bartczak and Galeski[28] investigated the interfacial shape during crystallization of one polymer in the presence of a second polymer in its molten state. When one polymer crystallized, its volume contracted; the other polymer (in the molten state) would flow into the gaps of spherulites of the crystallizing polymer. The interface changed from a flat form to one with many deep and branched "influxes" of the second polymer. The presence of "influxes" increases the interfacial strength mainly by increasing its area, and, as a consequence, there is improvement in the mechanical properties of the blends.

However, little research has been done on the formation of morphology introduced by the isothermal crystallization of PP in the PE melt. We previously reported the morphology, crystallization, and miscibility of these blends.[29,30] In this article, the mechanical properties of PE–PP blends are reported, and the relationship among the time–temperature treatment, morphology, and mechanical properties will be discussed.

EXPERIMENTAL

Materials and Blend Preparation

A PP homopolymer was blended with two LLDPEs, an LDPE, an HDPE, and a VLDPE. Table I lists all the materials with code names and characteristics. The blends were mixed in an Axon BX-12 single-screw extruder (Axon Austra-

lia Pty. Ltd., Australia) with a Gateway screw diameter of 12.5 mm and an *L/D* ratio of 26:1. The operating temperature for the feeding zone, melting zone, compression zone, and die-end were 160, 200, 200, and 170°C, respectively. The screw speed was 80 rpm. Samples were extruded, from a flat strip die, as sheets with a width of 30 mm and a thickness of 0.2 mm. All the blends were in the proportion of PE:PP of 80:20 by mass.

Heat–Time Treatment of the Blends

The samples from the extruder were cut to size and clamped between aluminum sheets. Teflon sheets were placed in between the samples and aluminum sheets to avoid sticking and contamination of the samples. In a digital temperature-controlled oven (Contherm oven, Cat 2050–2400, Contherm Scientific Co., New Zealand), one set of samples was melted at 200°C for 10 min and cooled to 130°C (cooling time approximately 20 min), then isothermally treated at 130°C for 5 h. Afterward, the samples were removed from the oven to room temperature (22°C); this set of samples will be referred to as oven thermally treated samples. At 130°C, only the PP could crystallize and the PEs were in a molten state. PEs could only crystallize after the samples were removed from the oven. The second set of samples was melted at 200°C for 10 min and removed from the oven and allowed to cool to room temperature; this set of samples will be referred to as ambient-cooled samples. These two sets of samples were later used in tensile tests and differential scanning calorimetry measurements.

Tensile Property Test

Tensile tests were performed using an Instron universeral testing system (Model 4465, Instron Pty. Ltd., Australia) at ambient (22°C). The measurements were made at a crosshead speed of 50 mm min^{-1}. Five measurements were recorded for

each blend and the average values were calculated and reported.

Differential Scanning Calorimetry (DSC)

A Perkin–Elmer DSC7 was used under a nitrogen purge. Samples of around 5 mg were weighed into aluminum pans and sealed with a crimper. DSC-treated samples were prepared in a DSC at 130°C for 5 h after melting at 200°C for 5 min. The fourth set of samples was melted at 200°C for 5 min followed by $10°C \ min^{-1}$ cooling to 40°C. These will be referred to as $10°C \ min^{-1}$-cooled samples. Melting of all treated samples was performed by heating the specimens from 40 to 200°C at a scan rate of $10°C \ min^{-1}$.

Hot-Stage Optical Microscopy with Polarized Light (HSOM)

HSOM was performed using a Nikon Labophot II microscope with a Mettler FP90 hot stage. Images were captured using a Sony video camera and video monitor connected to a Macintosh 7500 computer with IPLab image analysis software. Specimens of 20-μm thickness were prepared with a microtome. The films were melted at 200°C for 5 min, then cooled to an isothermal crystallization temperature between 124 and 130°C. To compare the morphology of the blends under the microscope and in the oven, one set of films was treated in an oven after being placed between glass slides and coverslips using the same procedure described for oven thermally treated samples. The final morphology of oven-treated films was analyzed by optical microscopy. The melting time at 200°C in the oven was longer than those in the DSC and on the hot-stage to ensure removal of the previous thermal history, because the heat transmission in the oven is not as efficient as for the DSC and on the hot-stage. In addition, a larger amount of samples was used in the oven for the tensile test. Hence, a longer time was needed to completely melt the samples.

Scanning Electron Microscopy (SEM)

The films crystallized under HSOM were also examined by SEM. The films were etched for 1 h at ambient in a solution of 1% wt/vol potassium permanganate with a mixture of 10 vol concentrated sulfuric acid and 4 vol of orthophosphoric acid as a solvent. The etched samples were vacuum-dried before being gold-coated in an SPI sputter coater. To prevent overheating, the coating was performed by coating the films in bursts of 20 s up to a cumulative time of 2 min. A JEOL JSM-35CF SEM with a secondary electron detector was used, operating at 20 kV.

RESULTS AND DISCUSSION

Tensile Properties

Figure 1 shows the tensile test results of pure polymers and the blends both after oven thermal treatment and ambient cooling. Values are at 95% confidence. The addition of PP to the PEs improved the Young's modulus and yield stress. The Young's modulus was increased after thermal treatment for all the materials except pure PP. The most significant increases were for the blends with two LLDPEs. Considering the experimental errors, the yield strength was unchanged for most of the blends and pure polymers except for the PP, VLDPE, HDPE–PP, and VLDPE–PP blends. The effect of thermal treatment on the yield strength was not as significant as that on the modulus and strain at break. Since the work by Schotland[31] on pure PP, the conclusion that thermal treatment increases the tensile properties (modulus and yield strength) of pure polymers has been widely accepted. In this study, the reason for the decreased strain at break and strength for the PP samples was that thermally treated PP samples broke before they reached a maximum value. The reasons for the decreased yield stress in the VLDPE and HDPE–PP blends after thermal treatment are complex because of the larger crystal size, more complete phase separation, and weak interfacial boundaries after annealing. Further study is needed to explain these behaviors.

It is interesting to note that the yield strength of both PP and VLDPE decreased after the thermal treatment, but that the thermal treatment improved the yield strength of the VLDPE–PP blend by almost 20%. The improvement in tensile properties with thermal treatment is more clearly shown in Figure 2. The Young's modulus and strain at break are clearly seen to increase for all the materials except pure PP. The Young's modulus and the strain at break increased by approximately 40% for the LLDPE1–PP and LLDPE2–PP blends and by approximately 20% for the VLDPE–PP blend, but by a smaller amount for the PP blends with LDPE and HDPE.
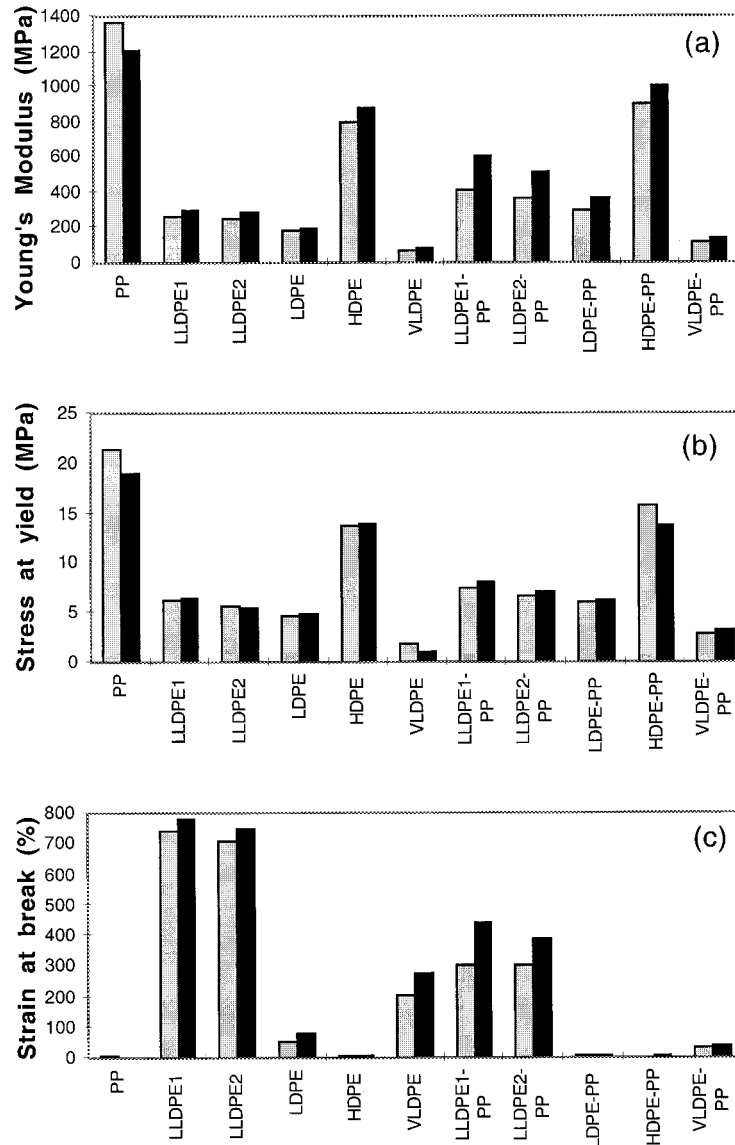
Figure 1 Tensile properties of thermal-treated and ambient-cooled samples: (a) Young's modulus; (b) yield stress; (c) strain at break. (■) Thermally treated; (▢) ambient cooling.

The reasons for these differences will be discussed later.

Crystal Structure Observed by Microscopy

Hot-stage optical microscopy showed the different PP spherulite structures in the various blends. Figure 3(a,b) demonstrates that similar morphologies for the pure PP were obtained for both specimens crystallized on the hot-stage and in the oven; the latter was then used for the tensile measurements. Figure 4(a,b) shows that the PP spherulites grow diffusely in the liquid LLDPE under isothermal crystallization. The PP is soluble in molten LLDPE and the crystals grow from the homogeneous solution of PP and LLDPE. The growth rate of the PP spherulite in the LLDPE melt was observed to be very slow. The number of nuclei stopped increasing after an initial period (from several minutes to around 20 min depending on the crystallization temperature) and remained constant thereafter. The size of the spherulites increased very slowly with time. It was also observed that the spherulites of PP in the LLDPEs were not as perfect as those for pure
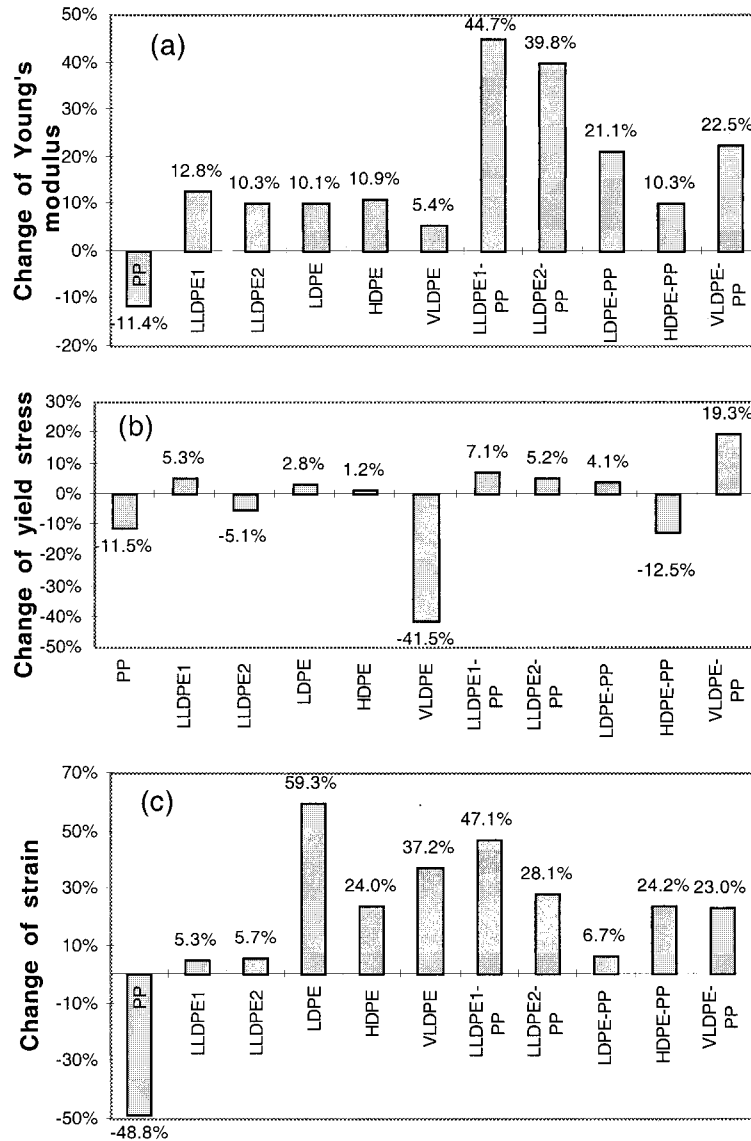
Figure 2 Change of (a) Young's modulus, (b) yield stress, and (c) strain at break of thermally treated samples compared with ambient-cooled samples.

PP, as shown in Figure 4(a,b), because of the small proportion of PP present and hindrance from molten LLDPE.

Furthermore, the PP was not as soluble in LLDPE1 as in LLDPE2 since some droplets were observed in LLDPE1. LLDPE1 is more viscous than is LLDPE2 since LLDPE1 has a lower melt-flow index. PP should be more miscible with LL-DPE2 because of the lower viscosity of LLDPE2 and closer match in their viscosities. Therefore, PP appeared as sharper crystals in LLDPE2 due to complete solubility. The higher melt viscosity also slowed the rate of crystallization.[29,30] The growth of PP spherulites was slower in LLDPE1 compared with the growth in LLDPE2.

After 17 hours, the growth of PP spherulites ceased. The blends were further cooled and the diffuse spherulite-matrix morphology formed in the LLDPE–PP blends [Fig. 5(a,b)]. These images were recorded at ambient. The small crystals are LLDPE, and the large bright spherulites are PP crystals. The PP spherulites were diffusely crystallized and the diffuse spherulite structure had a large surface area with LLDPEs. Figure 5(a,b) also shows similar morphologies for the LLDPE–PP blends crystallized in the oven and under the hot-stage microscope.

In the blends with HDPE, LDPE, and VLDPE (Fig. 6a–c), the PP crystallized as phase-separated droplets, in which almost pure PP was
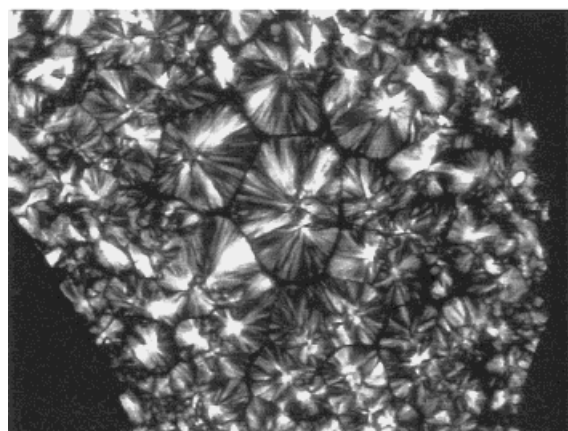
Figure 3 PP spherulites: (a) after isothermal crystallization at 130°C for 120 min; (b) with an oven thermally treated history. Images were recorded at ambient temperature; magnification ×100.

The images in Figure 6 are clearer compared with those in Figure 7. Since in Figure 6 the images were recorded at 130°C, the PEs were in the molten state and, therefore, they appeared as a dark background under polarized optical microscopy, whereas in Figure 7, the images were recorded at ambient and the PE matrixes were also crystalline.

DSC Results

The DSC melting curves for pure PP with different thermal histories are shown in Figure 8. The DSC-treated specimens showed similar melting behavior as that of the oven-treated specimens. The shape of the PP endotherm of the untreated sample was simple. After thermal treatment, the PP melting peak shifted to a higher temperature. Small shoulders appeared in the lower tempera-
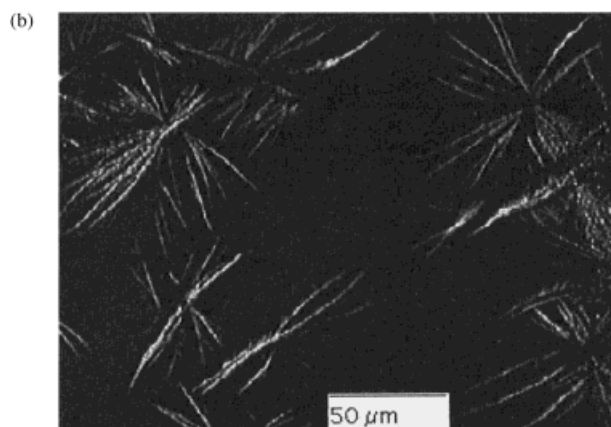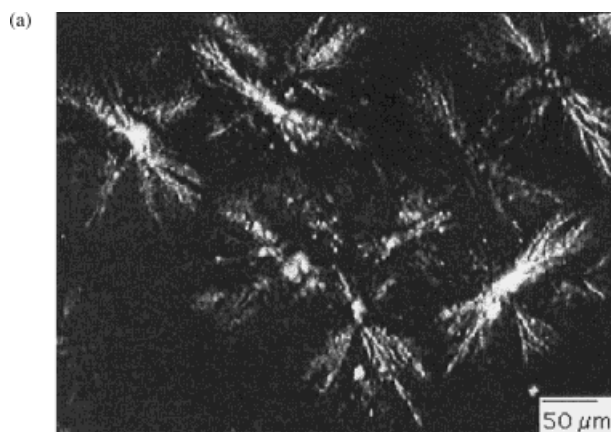

Figure 4 (a) PP spherulites in a blend of LLDPE1 (80%)–PP (20%) after isothermal crystallization at 130°C for 180 min, magnification ×100; (b) PP spherulites in a blend of LLDPE2 (80%)–PP (20%) after isothermal crystallization at 124°C for 100 min, magnification ×200.

present. The crystallization within droplets was completed in several minutes. The crystallization rate was observed to be similar to that of pure PP. The shape and size of the droplets and the crystal structure did not change anymore after an initial several minutes (3–5 min). A further contribution to the PP crystallization was the appearance of more droplets. More PP separated from the melt and more nuclei formed with time.

The PP droplets were smaller in VLDPE as shown in Figure 6(c). Therefore, it would appear that PP must be more soluble in VLDPE. In Figure 6(b), the PP droplets were larger than those in the VLDPE and LDPE, indicating that the PP had a low solubility in the HDPE. After the PEs crystallized, droplet-matrix structures were formed in these blends. The PEs formed a continuous phase while PP appeared as isolated domains in the PE matrix [Fig. 7(a–c)]. Figures 6 and 7 also show that similar morphologies formed during hot-stage microscopy and oven treatment.
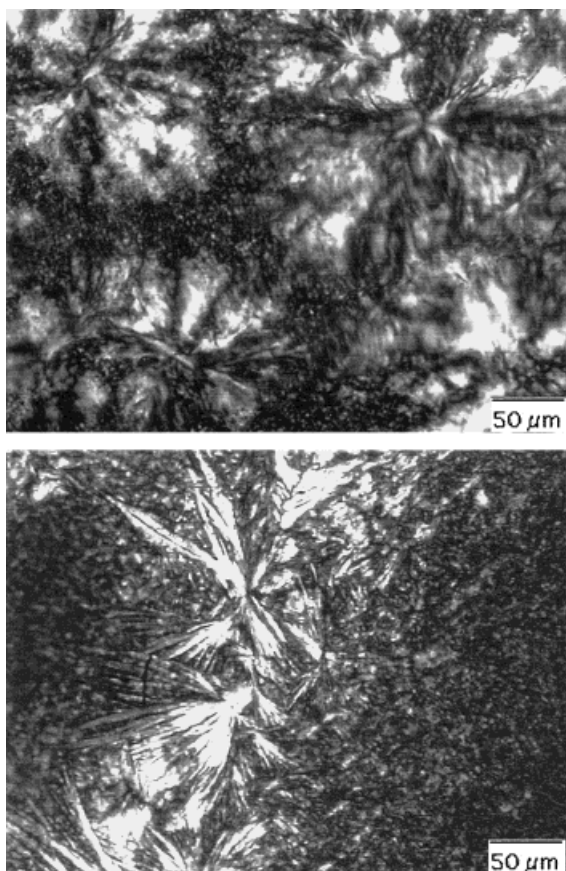
Figure 5 Diffuse PP spherulites in (a) LLDPE1 matrix and (b) LLDPE2 matrix after being treated in an oven at 130°C for 5 h. Images were recorded at ambient; magnification ×100.

ture part and the PP melting peak became broader. Poussion et al.[32] annealed PP at 125°C for different lengths of time and studied its crystalline structure and melting behavior. They found that this temperature favored molecular mobility in the amorphous phase, and the motion of the chains led to a more stable thermodynamic position. The better organization of the amorphous chains led to the formation of zones in which the molecular arrangement was close to the crystal organization. The shoulders in the PP melting peak are probably due to the fusion of such microcrystalline zones, indicating a microstructural evolution generated by the heat treatment.

Another possibility is that the shoulders may be formed from the crystallization during cooling after annealing because crystallization of PP at a high temperature such as 130°C could be incomplete. However, the crystallization of pure PP at

130°C was rapid. The microscopic images did not show a significant difference in the appearance of PP recorded at 130°C to that recorded at ambient after isothermal crystallization at 130°C for 2 h. This phenomenon could happen in the blends be-
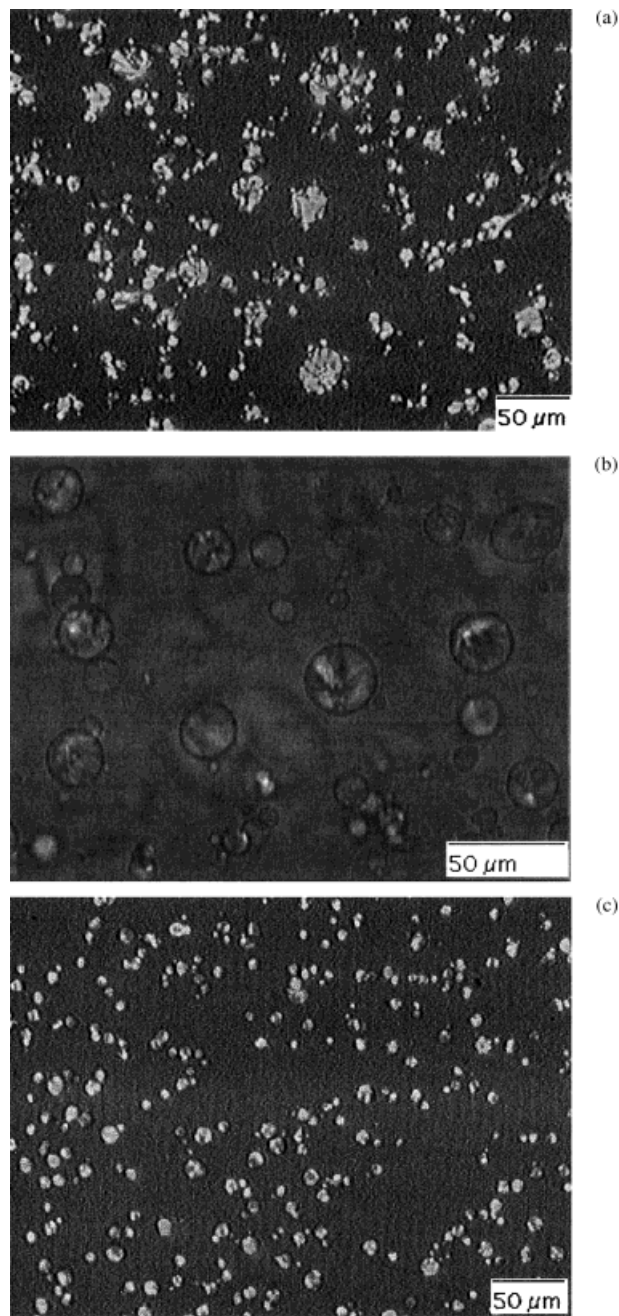

Figure 6 PP droplets in a blend of (a) LDPE (80%)–PP (20%) at 126°C after 115 min, magnification ×100; (b) HDPE (80%)–PP (20%) at 130°C after 20 min, magnification ×100; and (c) VLDPE (80%)–PP (20%) at 124°C after 3 min, magnification ×100.
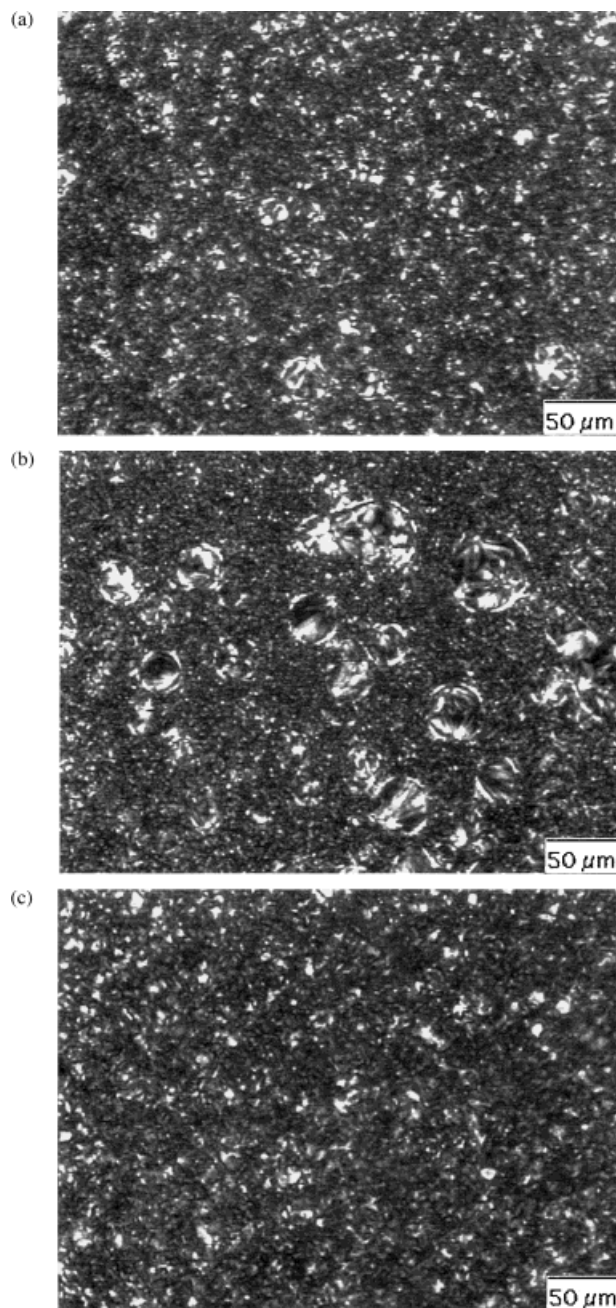
Figure 7 Dispersed PP droplets in the matrix of (a) LDPE, (b) HDPE, and (c) VLDPE after being treated in an oven at 130°C for 5 h. Images were recorded at ambient; magnification ×100.

Figure 8 DSC curves of the PP with various thermal histories: (a) DSC-treated; (b) oven thermally treated; (c) ambient-cooled; (d) 10°C min^{-1}-cooled.

thermally treated specimen. The melting temperature of a specimen cooled at 10°C min^{-1} was higher than that of an ambient-cooled specimen since fast cooling (ambient cooling) formed small crystals. The melting curves of the LLDPE1–PP blend with the same heat treatments were the same as those of the LLDPE2–PP blend. In Fig-

cause PP crystallized slowly in the blends, especially in the LLDPE–PP blends.

Figure 9 shows DSC melting curves of the LLDPE2–PP blend with various heat treatments. The melting peak of LLDPE2 did not change in all cases. Small shoulders appeared at the lower-temperature region in the PP melting peak for the
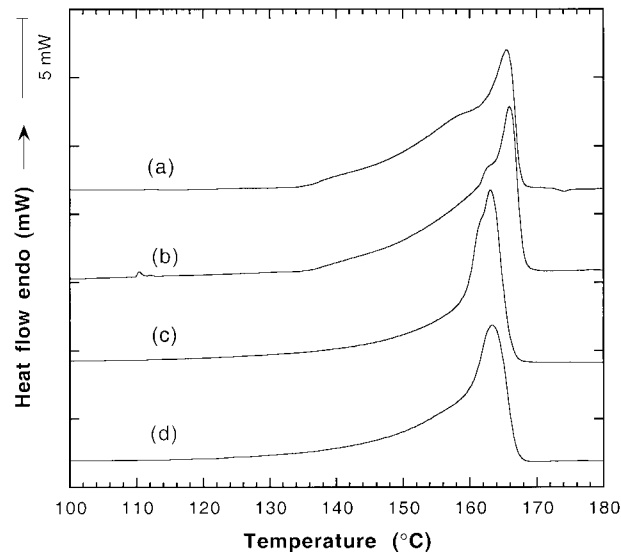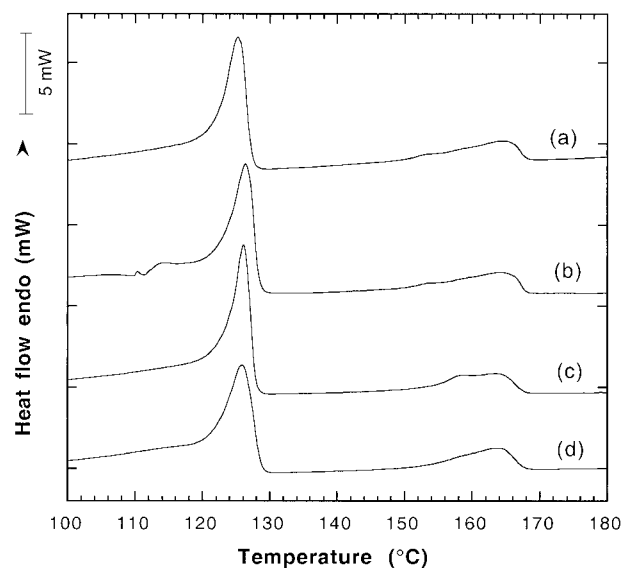

Figure 9 DSC curves of the LLDPE2 (80%)–PP (20%) blend with (a) DSC-treated, (b) oven thermally treated, (c) ambient-cooled, and (d) 10°C min^{-1}-cooled thermal histories.

Figure 10 DSC curves of the LDPE (80%)–PP (20%) blend with (a) DSC-treated, (b) oven thermally treated, (c) ambient-cooled, and (d) 10°C min^{-1}-cooled thermal histories.
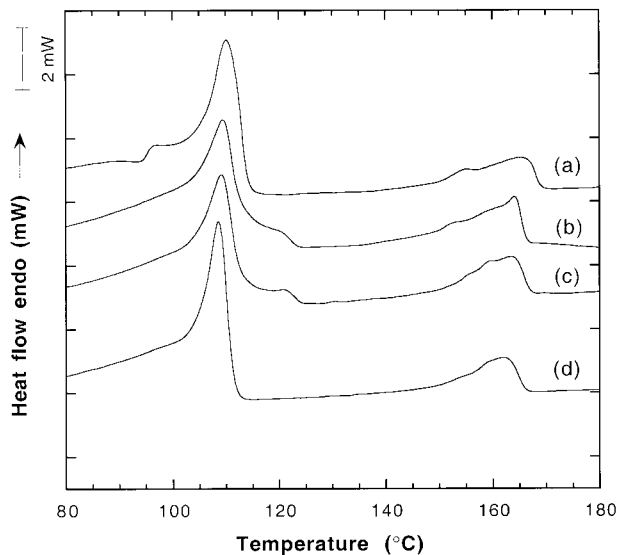

Figure 11 DSC curves of the HDPE (80%)–PP (20%) blend with (a) DSC-treated, (b) oven thermally treated, (c) ambient-cooled, and (d) 10°C min^{-1}-cooled thermal histories.

ure 10, the 10°C min^{-1} cooling also showed a simple PP melting endotherm. However, the ambient-cooled samples displayed a higher PP melting peak than that of the specimen prepared at 10°C min^{-1} cooling. This was due to the recrystallization of the PP during heating. Isothermal crystallization at 130°C showed the highest melting temperature. If PP was not completely crystalline at this temperature, the shoulder would have formed during the rapid cooling. Again, in Figure 11, the ambient-cooled sample showed the second highest melting peak for the PP because of recrystallization.

A third melting peak was observed in the VLD-PE–PP blend (Fig. 12). This peak, similar to the melting temperature of LLDPE, appeared between 122 and 125°C and was not observed both in pure VLDPE and pure PP. It may be caused by the melting of less branched molecules separated from VLDPE after blending with PP because the less branched molecules should be more miscible with PP. In other words, less branched molecules were extracted into the PP during blending and these molecules dissolved in the PP in the melt. On cooling, the less branched molecules separated from the PP solution and melted separately at a higher temperature.

The experimental melting enthalpy was used to calculate the crystallinity of PP (Table II). An enthalpy of fusion of 209 J g^{-1} for PP was used.[33]
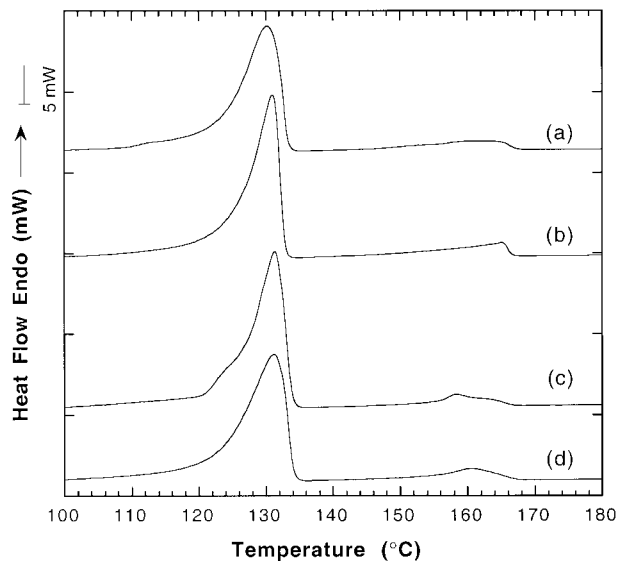
The crystallinity of PP was found to increase after thermal treatment. Excess heat of fusion was used to indicate the crystallinity change of the PEs and the blends with a particular thermal history compared with samples with 10°C min^{-1} cooling. For pure PEs, the excess heat of fusion is
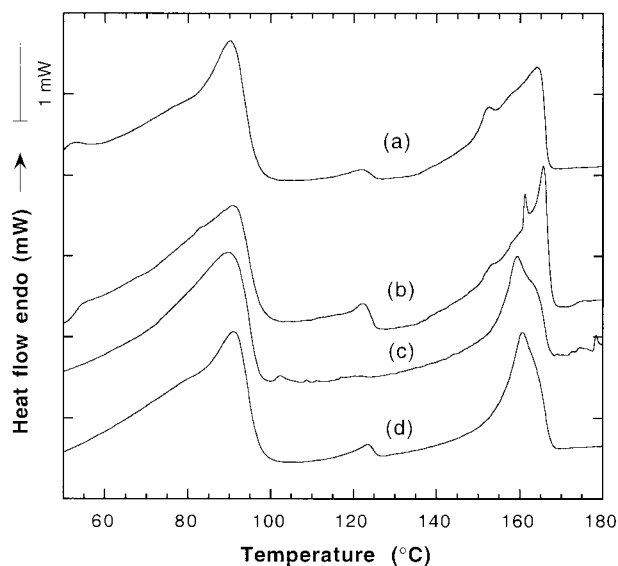

Figure 12 DSC curves of the VLDPE (80%)–PP (20%) blend with (a) DSC-treated, (b) oven thermally treated, (c) ambient-cooled, and (d) 10°C min^{-1}-cooled thermal histories.

Table II   Crystallinity of PP in the Pure PP and the Blends with Various Thermal Histories

| Sample	DSC-Treated	Oven-Treated	Ambient-Cooled	10°C min^{-1}-Cooled
PP	0.52	0.53	0.48	0.46
LLDPE1–PP	0.46	0.47	0.38	0.36
LLDPE2–PP	0.45	0.46	0.41	0.40
LDPE–PP	0.45	0.49	0.43	0.37
HDPE–PP	0.45	0.50	0.36	0.38
VLDPE–PP	0.53	0.52	0.41	0.46

the difference between the heat of fusion of PE with a particular thermal history and the heat of fusion of PE with 10°C min^{-1} cooling. For the blends, the excess enthalpy (ΔH_c^e) is given by eq. (1):

$$\Delta H_c^e = \Delta H_c - \sum w_i \Delta H_{c,i} \qquad (1)$$

where ΔH_c is the heat of fusion of the PEs and PP in the blends; w_i, the weight percentage of the PEs and the PP in the blends; and $\Delta H_{c,i}$, the heat of fusion of the pure PE and PP with 10°C min^{-1} cooling history. The crystallinity of PP remained the same as for pure PP after blending with VLDPE but decreased after blending with all other PEs. Furthermore, in Table III, it can be seen that the crystallinity decreased in the blends of LDPE–PP and HDPE–PP compared with the pure polymers. Thermal treatment improved the

Table III   Excess Heat of Fusion for PEs and Blends with Particular Thermal History over Polymers with 10°C min^{-1} Cooling

Sample	DSC-Treated (J g^{-1})	Oven-Treated (J g^{-1})	Ambient-Cooled (J g^{-1})	10°C min^{-1}-Cooled (J g^{-1})
LLDPE1	14.53	14.71	2.54	0.00
LLDPE2	12.77	15.38	6.09	0.00
LDPE	−12.27	−2.43	8.36	0.00
HDPE	−11.39	−7.69	−8.26	0.00
VLDPE	12.17	9.07	−1.79	0.00
LLDPE1–PP	13.41	17.38	8.53	7.02
LLDPE2–PP	2.35	9.02	1.99	3.30
LDPE–PP	2.32	1.76	−8.12	−6.93
HDPE–PP	−11.03	−9.97	−3.67	−7.52
VLDPE–PP	5.48	3.23	−4.52	−0.70
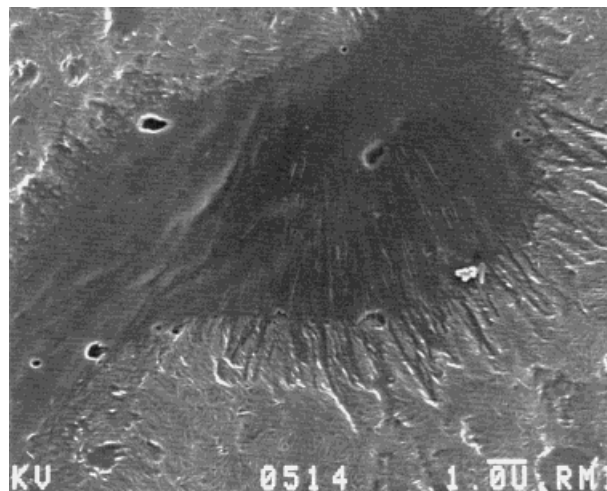
Figure 13 SEM of the LLDPE1 (80%)–PP (20%) blend; magnification ×6000.

crystallinity of PP, LLDPE, and VLDPE, but not of HDPE and LDPE. However, the overall crystallinity of the LDPE–PP blend increased after annealing but not of the HDPE–PP blend. The decreased crystallinity contributed negatively to the tensile properties of the thermally treated HDPE–PP blends.

SEM Results

Figure 13 shows a fibrous structure of PP spherulites and small PP droplets of less than 1 μm diameter in the LLDPE1 matrix, located in the upper-left-hand side of the image. The fibrillar structure of the PP could penetrate the LLDPE phase. The PE was distributed in between and around the fibrillar of the PP spherulites. Figure 14 shows the larger PP droplets with rounded and smooth edges in the HDPE matrix. The SEM results are in accordance with optical microscopic observations.

Correlation Among Morphology, Crystallization, and Tensile Properties

The DSC and HSOM results show that oven-treated specimens in a large scale had the same morphologies as those of specimens crystallized under HSOM and the same crystallization characteristics as those of the DSC-treated specimens. Therefore, the morphology, crystallization, and mechanical properties of the blends can be compared.

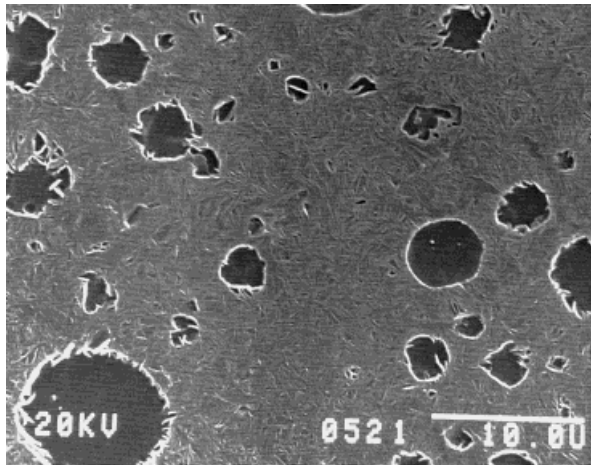The three elements that dictate the mechanical properties of polymer blends are the total crystal-

Figure 14 SEM of the HDPE (80%)–PP (20%) blend; magnification ×2400.

linity, morphology, and interfacial properties. Deterioration of the mechanical properties is a result of the two-phase structure of the blends. The thermal treatment improves the overall crystallinity of the blends and the perfection of the PP crystals and sometimes the perfection of PE crystals and, as a consequence, provides an enhancement of the modulus as well as the strength. Thermal treatment also promotes the intercrystalline links (adhesion at the interface). This was also reported by Varin and Djokovic.[19] Their SEM images showed that there were "bridging" bonds between the PP and HDPE phases in the annealed samples, which were not found in the unannealed samples. Low mechanical properties of the polyolefin blends are a result of poor interfacial adhesion and poor stress transfer between the phases. Upon thermal treatment, the entanglements of PP and PE increased with time. The improved interfacial adhesion should provide a contribution to the improved tensile properties of the treated samples.

An increase in crystallinity would display an increased modulus but lower strain at break due to thicker lamellae. Annealing is expected to promote both the crystallinity and the intercrystalline links. Annealing also causes greater phase separation in immiscible blends since the degree of phase separation increases with annealing time, which may reduce the interfacial adhesion. If the melting temperature has increased with the thermal treatment, then it means that the lamellae are thicker and an increased modulus is expected. From Table III, the crystallinity was increased for all the blends except for the

HDPE–PP blend, but the modulus improved after the thermal treatment for all the blends. Pure HDPE had reduced crystallinity as did its blend after thermal treatment, but the PP phase always had greater crystallinity when either DSC- or oven-treated. PP has a much higher modulus than that of HDPE (approximately 1.6 times); therefore, the PP droplets will be like a stiff filler in the PE and increase the modulus and maybe the yield stress. Twenty percent of the filler would be expected to have a significant effect. The modulus of the composite (E_c) is given by eq. (2):

$$E_c = aV_fE_f + (1 - V_f)E_p \qquad (2)$$

where f is the filler; p, the polymer (matrix phase); and a, an efficiency factor dependent on the interfacial adhesion. V_f is the volume fraction of the filler and E_f and E_p are the moduli of the filler and polymer, respectively. In addition, it seems that the improved interfacial adhesion upon annealing dominated the properties since the strain at break in the HDPE–PP blend was also greater after thermal treatment.

Formation of a diffuse spherulite-matrix morphology plays a significant role in the improvement of the tensile properties of the LLDPE–PP blends. This morphology improved the bonding of the PP and LLDPE phases by the presence of diffusely crystallized PP spherulites and a fibrillar structure. Not only the modulus and yield stress but also the ductility was improved significantly after thermal treatment of these blends. This is in contrast to previous studies.[19,25,27] All studies on annealing reported decreased ductility even though most of them showed improved modulus and strength. The method of thermal treatment plays an important role in the formation of a different morphology and, hence, the performance of the blends. Blom et al.[25] annealed samples at 75°C; the mobility of both PP and PE was limited at this temperature. Zhou and Hay[27] annealed blends at 130°C, but the specimens were previously quenched in water. At this temperature, only the PE was in the molten state and PP was in the solid state. The evolution in the PP crystalline structure and interfacial structure between PP and PE was less efficient. In our study, the blends were cooled from the melt and then held at 130°C to allow the PP to crystallize first. A similar method was employed by Varin and Djokovic in their study.[19] However, decreased elongation after annealing was observed. This could be

due to that different blends (HDPE–PP) were used in their study and so a droplet-matrix morphology was achieved. Only the diffuse spherulite-matrix morphology exhibited better strain properties after annealing, and this morphology only developed in the LLDPE–PP blends because PP was miscible with LLDPE at elevated temperatures.[29,30] The diffusion of PP spherulites into the PE liquid was possible and PP could crystallize as spherulites in LLDPE. In other blends, the phase separation occurred before the crystallization started, and PP could only crystallize in phase-separated domains. The phase boundary was smooth as shown in Figure 14. The bonding between PP and PEs was much weaker in the blends of HDPE–PP, LDPE–PP, and VLDPE–PP.

PP has a very large surface with LLDPE, so this will increase the strength. Its fibrous crystals (Fig. 13), penetrating into the LLDPE, reinforced the LLDPE like a stiff fibrous filler (the Young's modulus of the PP was five to six times of that of the LLDPEs). Clearly, the much greater increase in the modulus and strain at break for the LLDPE–PP blends compared with all the other blends demonstrates that this unique solution-grown morphology observed by optical microscopy and the fibrillar structure by SEM provides mechanical properties analogous to those in a fibrous-reinforced composite.

It is noted that the VLDPE–PP blend displayed greater improvement in tensile properties after thermal treatment over the LDPE–PP and HDPE–PP blends. This is due to the much smaller domain size of PP in VLDPE–PP blend as shown in Figure 6(c). Long et al.[34] studied the dependence of the mechanical properties on particle size. They found that the Young's modulus and yield strength decreased with increasing particle size. PP droplets were large in the HDPE–PP blend [Fig. 6(b)]. After HDPE crystallized, the PP droplets were still apparent in the HDPE matrix [Fig. 7(b)]. In the VLDPE–PP blend [Fig. 7(c)], PP droplets were almost indistinguishable among the VLDPE crystals. In the LDPE–PP blend, both large and small droplets were present. Small particles have better adhesion with the matrix simply because of an increased interfacial area. However, this system is not as strong as is the LLDPE–PP system. In the LLDPEs, diffuse PP spherulites grow into the PE phase. The PP fibrils branched out in all directions and sometimes connected fibrils from several spherulites, reinforcing the PE matrix. Obviously, this system is much stronger than is a particle–matrix system.

CONCLUSIONS

Thermal treatment improved the tensile properties for a range of PE–PP blends by improving the adhesion between PP and PE and increasing the overall crystallinity. In particular, in the partially miscible blends of LLDPE–PP, a diffuse spherulite-matrix morphology and fibrillar structure were revealed by polarized optical microscopy and SEM, respectively. The PP spherulitic structure extending in all directions reinforced the PE phase like a fibrous filler. This morphology improved the interfacial energy between PP and PE greatly and, hence, the tensile properties improved significantly in these blends. In other blends, the improvements of tensile properties were not as significant as in the LLDPE–PP blends because a droplet-matrix morphology was formed. The size of the dispersed phase is also an important factor that controls the mechanical properties. Small particles in the VLDPE–PP blend providing better interfacial adhesion with the matrix displayed superior performance.

REFERENCES

1. Deanin, R. D.; Chung, C.-H. In Handbook of Polyolefins—Synthesis and Properties; Vasile, C.; Seymour, R. B., Eds.; Marcel Dekker: New York, 1993; pp 779–798.
2. Noel, O. F., III; Carley, J. F. Polym Eng Sci 1975, 15, 117.
3. Lovinger, A. J.; Williams, M. L. J Appl Polym Sci 1980, 25, 1703.
4. Gupta, A. K.; Gupta, V. B.; Perters, R. H.; Harland, W. G.; Berry, J. P. J Appl Polym Sci 1982, 27, 4669.
5. Greco, R.; Mucciariello, G.; Ragosta, G.; Martuscelli, E. J Mater Sci 1980, 15, 845.
6. Robertson, R. E.; Paul, D. R. J Appl Polym Sci 1973, 17, 2579.
7. Deanin, R. D.; Sansone, M. F. ACS Div Polym Chem Polym Prepr 1978, 19, 211.

8. Lee, J.; O. Kim, B. K.; Ha, C. S.; Song, K. W.; Lee, J. K.; Cho, W. J. Polymer (Korea) 1994, 18, 68.

9. Nolly, E.; Barlow J. W.; Paul, D. R. Polym Eng Sci 1980, 20, 364.

10. Teh, J. W. J Appl Polym Sci 1983, 28, 605.

11. Liang, J. Z. Suoliao 1995, 24, 10.

12. Dumoulin, M. M.; Farha, C.; Utracki, L. A. Polym Eng Sci 1984, 24, 1319.

13. Dumoulin, M. M.; Carreau, P. J. Polym Eng Sci 1987, 27, 1627.

14. Yeh, P. L.; Birley, A. W. Plast Rubb Process Appl 1985, 5, 249.

15. Muller, A. J.; Latorre, C.; Mendez, G.; Rotino, J.; Rojas J. L. ANTEC 1994, 2418.

16. Lee, Y. K.; Jeong, Y. T.; Kim, K. C.; Jeong, H. M.; Kim, B. K. Polym Eng Sci 1991, 31, 944.

17. Zhu, W.; Zhang, X. Q.; Feng, Z. L.; Huang, B. T. J Macromol Sci-Phys B 1996, 35, 795.

18. Sawatari, C.; Satoh, S.; Matsuo, M. Polymer 1990, 31, 1456.

19. Varin, R. A.; Djokovic, D. Polym Eng Sci 1988, 28, 1477.

20. Teh, J. W.; Rudin, A. Adv Polym Technol 1994, 13, 1.

21. Bains, M.; Balke, S. T. Polym Eng Sci 1994, 34, 1260.

22. Bartllett, D. W.; Barlow, J. W.; Paul, D. R. J Appl Polym Sci 1982, 27, 2351.

23. Rizzo, G.; Spadaro, G. Eur. Polym J 1988, 24, 303.

24. Spadaro, G.; Rizzo, G. Eur Polym J 1989, 25, 1189.

25. Blom, H. P.; Teh, J. W.; Rudin, A. J Appl Polym Sci 1995, 58, 995.

26. Lin, G. X.; Wenig, W.; Petermann, J. Angew Makromol Chem 1998, 255, 33.

27. Zhou, X. Q.; Hay, J. N. Polymer 1993, 34, 4710.

28. Bartczak, Z.; Galeski, A. Polymer 1986, 27, 544.

29. Li, J.; Shanks, R. A.; Long, Y., submitted for publication in Polymer.

30. Shanks, R. A.; Li, J.; Long, Y. Polymer, 2000, 41, 2133.

31. Schotland R. S. Polym Eng Sci 1966, 6, 244.

32. Poussin, L.; Bertin, Y. A.; Parisot, J.; Brassy, C. Polymer 1998, 39, 4261.

33. Aggarwai, S. L. In Polymer Handbook, 2nd ed.; Brandrup, J.; Immergut, E. H., Eds.; John Wiley & Sons, New York 1975; Vol. 24.

34. Long, Y.; Stachurski, Z. H.; Cherry, B. W.; Shanks, R. A. In 8th International Conference on Deformation Yield and Fracture of Polymers, Cambridge, UK, 8–11 April 1991; Vol. 121, pp 1–4.